Syntheses and Spectroscopic and Electrical Properties of $[W(C_3S_5)_3]^{2-}$ and $[Mo(C_3S_5)_3]^{2-}$ Anion Complexes and Their Oxidized Species and X-ray Crystal Structures of $[NBu^n{}_4]_2[W(C_3S_5)_3]$, $[NBu^n{}_4]_2[Mo(C_3S_5)_3]$, and $[Fe(C_5Me_5)_2][W(C_3S_5)_3]$

Gen-etsu Matsubayashi,* Katsuji Douki, Hatsue Tamura, and Motohiro Nakano

Institute of Chemistry, College of General Education, Osaka University, Toyonaka, Osaka 560, Japan

Wasuke Mori

Department of Chemistry, Faculty of Science, Osaka University, Toyonaka, Osaka 560, Japan

Received July 20, 1993[⊗]

$[NBu^n{}_4]_2[W(C_3S_5)_3]$ (**1**) and $[NBu^n{}_4]_2[Mo(C_3S_5)_3]$ (**2**) [$C_3S_5{}^{2-}$ = 4,5-dimercapto-1,3-dithiole-2-thionate(2–)] were prepared. Single-crystal X-ray structure analyses revealed a distorted trigonal prismatic coordination around the metal atom for both the anion moieties. They were oxidized by $[Fe(C_5Me_5)_2][BF_4]$ to afford $[Fe(C_5Me_5)_2][W(C_3S_5)_3]$ (**3**) and $[Fe(C_5Me_5)_2][Mo(C_3S_5)_3]$ (**4**), respectively. A single-crystal structure analysis of **3** revealed that the complex consists of the $[Fe(C_5Me_5)_2]^+$ cation and the $[W(C_3S_5)_3]^-$ anion with almost a regular trigonal prismatic geometry around the tungsten atom and that the anion moieties are arranged one-dimensionally through sulfur–sulfur nonbonded contacts in the crystal phase. Complexes **1** and **2** reacted with iodine, $[Fe(C_5H_5)_2][PF_6]$, or $[TTF]_3[BF_4]_2$ ($TTF^{+\bullet}$ = the tetrathiafulvalenium radical cation) to afford oxidized species $[NBu^n{}_4]_x[M(C_3S_5)_3]$ (M = W, Mo; x = 0.05–0.4). One-electron-oxidized complexes **3** and **4** exhibit electrical conductivities of 6.0×10^{-5} and 1.1×10^{-4} S cm^{-1}, respectively, and the further oxidized species $1 \times (10^{-3}–10^{-1})$ S cm^{-1} at room temperature as compacted pellets. Redox potentials of **1** and **2** were determined. Electronic absorption, IR, ESR spectra, and magnetic properties of these tungsten and molybdenum complexes are discussed. Crystal data: **1**, orthorhombic, $Pca2_1$, a = 32.905(7) Å, b = 10.779(2) Å, c = 16.398(3) Å, V = 5816(2) Å^3, Z = 4, 4847 reflections, R = 0.049; **2**, orthorhombic, $Pca2_1$, a = 32.881(1) Å, b = 10.788(5) Å, c = 16.382(9) Å, V = 5811(5) Å^3, Z = 4, 3303 reflections, R = 0.087; **3**, triclinic, $P\bar{1}$, a = 12.150(2) Å, b = 14.756(1) Å, c = 11.9041(9) Å, α = 110.771(6)°, β = 97.087(8)°, γ = 83.84(1)°, V = 1975.7(4) Å^3, Z = 2, 9578 reflections, R = 0.040.

Introduction

Many metal complexes with the 4,5-dimercapto-1,3-dithiole-2-thionate(2–) ligand ($C_3S_5{}^{2-}$) have been extensively studied,[1–4] since they become good electrical conductors and some of them are known as superconductors.[3–6] High electrical conductivities are caused by electron-conduction pathways which are constructed with two- or three-dimensional molecular interactions through sulfur–sulfur contacts of the ligands in the solid state. Although bulky molecules may be often considered to be ineffective for their packings in the solid state, C_3S_5–metal complexes with bulky geometries are expected to afford new multidimensional conduction pathways through sulfur atoms of this sulfur-rich ligand. Several bulky C_3S_5–metal complexes as conductors have been reported.[7–13] Oxidized species of $[V(C_3S_5)_3]^{2-}$ complexes were found to behave as semiconductors.[7–9,12] Thus, oxidized octahedral $[M(C_3S_5)_3]$ complexes are expected to become new conductors having unique effective electron-conduction pathways.

This paper reports electrochemical and spectroscopic properties of $[M(C_3S_5)_3]^{2-}$ (M = Mo, W) anion complexes and electrical conductivities of their oxidized species, together with X-ray crystal structures of $[NBu^n{}_4]_2[M(C_3S_5)_3]$ (M = Mo, W) and $[Fe(C_5Me_5)_2][W(C_3S_5)_3]$. A part of this work has already appeared as a preliminary report.[14]

Experimental Section

Materials. 4,5-Bis(benzoylthio)-1,3-dithiole-2-thione,[15] $[Fe(C_5H_5)_2][PF_6]$, $[Fe(C_5Me_5)_2][BF_4]$,[8] and tris(tetrathiafulvalenium) bis(tetrafluoroborate) ($[TTF]_3[BF_4]_2$)[16] were prepared according to the literature.

Preparations of $[NBu^n{}_4]_2[W(C_3S_5)_3]$ (1) and $[NBu^n{}_4]_2[Mo(C_3S_5)_3]$ (2). All the following reactions were performed under a nitrogen atmosphere. 4,5-Bis(benzoylthio)-1,3-dithiole-2-thione (810 mg, 2.0 mmol) was dissolved in an ethanol (15 mL) solution containing sodium metal (260 mg, 11 mmol). To the resulting solution of $Na_2[C_3S_5]$ was added with stirring an ethanol (10 mL) solution of WCl_6 (790 mg, 2.0 mmol) and $[NBu^n{}_4]Br$ (430 mg, 1.4 mmol). The solution was allowed to stand overnight to give black microcrystals, which were recrystallized from a mixture of ethanol and dichloromethane to afford black plates of **1**. Yield: 480 mg (20% yield). Anal. Calcd for $C_{41}H_{72}N_2S_{15}W$: C, 39.15; H, 5.77; N, 2.23. Found: C, 38.86; H, 5.64; N, 2.28.

Similarly, a reaction of $MoCl_5$ with $Na_2[C_3S_5]$ in methanol in the presence of $[NBu^n{}_4]Br$ gave black microcrystals of **2** (7% yield) together with a large amount of dark red crystals of $[NBu^n{}_4]_2[MoO(C_3S_5)_2]$,[17] as described previously.[14]

[⊗] Abstract published in *Advance ACS Abstracts*, November 15, 1993.

(1) Cassoux, P.; Interrante, L. V. *Comments Inorg. Chem.* **1991**, *12*, 47.
(2) Matsubayashi, G. *Heteroatom Chemistry*; Myu: Tokyo, 1991, Vol. 4, p 171.
(3) Cassoux, P.; Valade, L.; Kobayashi, H.; Kobayashi, A.; Clark, R. A.; Underhill, A. E. *Coord. Chem. Rev.* **1991**, *110*, 115.
(4) Olk, R.-M.; Olk, B.; Dietzsch, W.; Kirmse, R.; Hoyer, E. *Coord. Chem. Rev.* **1992**, *117*, 99.
(5) Kobayashi, A.; Kobayashi, H.; Miyamoto, A.; Kato, R.; Clark, R. A.; Underhill, A. E. *Chem. Lett.* **1991**, 2163 and references therein.
(6) Kobayashi, H.; Bun, K.; Naito, T.; Kato, R.; Kobayashi, A. *Chem. Lett.* **1992**, 1909.
(7) Matsubayashi, G.; Akiba, K.; Tanaka, T. *Inorg. Chem.* **1988**, *27*, 4744.
(8) Akiba, K.; Matsubayashi, G.; Tanaka, T. *Inorg. Chim. Acta* **1989**, *165*, 245.
(9) Broderick, W. E.; McGhee, E. M.; Godfrey, M. R.; Hoffman, B. M.; Ibers, J. A. *Inorg. Chem.* **1989**, *28*, 2902.
(10) Matsubayashi, G.; Yokozawa, A. *J. Chem. Soc., Chem. Commun.* **1991**, 68.
(11) Yokozawa, A.; Matsubayashi, G. *Inorg. Chim. Acta* **1991**, *186*, 165.
(12) Martin, J. D.; Canadell, E.; Batail, P. *Inorg. Chem.* **1992**, *31*, 3176.
(13) Matsubayashi, G.; Maikawa, T.; Nakano, M. *J. Chem. Soc., Dalton Trans.* **1993**, 2995.
(14) Matsubayashi, G.; Douki, K.; Tamura, H. *Chem. Lett.* **1992**, 1251.
(15) Valade, L.; Legros, J.-P.; Bousseau, M.; Cassoux, P.; Garbauskas, M.; Interrante, M. *J. Chem. Soc., Dalton Trans.* **1985**, 783.
(16) Wudl, F. *J. Am. Chem. Soc.* **1975**, *79*, 1962.

0020-1669/93/1332-5990$04.00/0

Preparations of $[\mathrm{Fe(C_5Me_5)_2}][\mathrm{W(C_3S_5)_3}]$ (3) and $[\mathrm{Fe(C_5Me_5)_2}][\mathrm{Mo(C_3S_5)_3}]$ (4). An acetonitrile (30 mL) solution containing **1** (500 mg, 400 μmol) and $[\mathrm{Fe(C_5Me_5)_2}][\mathrm{BF_4}]$ (330 mg, 800 μmol) was allowed to stand for 2 h at 40 °C. Dark blue crystals of **3** obtained were collected by filtration, washed with acetonitrile and diethyl ether several times, and dried in vacuo (83% yield). Anal. Calcd for $\mathrm{C_{29}H_{30}FeS_{15}W}$: C, 31.74; H, 2.75. Found: C, 31.69; H, 2.75. A similar reaction of **2** with $[\mathrm{Fe(C_5Me_5)_2}][\mathrm{BF_4}]$ in acetonitrile gave black solids of **4** (47% yield).[14]

Preparations of $[\mathrm{NBu^n_4}]_x[\mathrm{M(C_3S_5)_3}]$ (M = Mo, W; x = 0.05–0.4) (5–10). To an acetonitrile (10 mL) solution of **1** (20 mg, 16 μmol) was added with stirring an acetonitrile (2 mL) solution of iodine (13 mg, 48 μmol) to give a black precipitate. The mixture was further stirred for 30 min. The product of $[\mathrm{NBu^n_4}]_{0.15}[\mathrm{W(C_3S_5)_3}]$ (**5**) was separated by centrifugation, washed with acetonitrile and diethyl ether, and dried in vacuo (93% yield). Anal. Calcd for $\mathrm{C_{11.4}H_{5.4}N_{0.15}S_{15}W}$: C, 16.92; H, 0.67; N, 0.26. Found: C, 16.67; H, 0.77; N, 0.28.

An acetonitrile (10 mL) solution of **1** (20 mg, 16 μmol) was added with stirring to an acetonitrile (10 mL) solution of $[\mathrm{Fe(C_5H_5)_2}][\mathrm{PF_6}]$ (10 mg, 30 μmol) to afford a black precipitate of $[\mathrm{NBu^n_4}]_{0.4}[\mathrm{W(C_3S_5)_3}]$ (**6**). It was collected by centrifugation, washed with acetonitrile and diethyl ether, and dried in vacuo (38% yield). Anal. Calcd for $\mathrm{C_{15.4}H_{14.4}N_{0.4}S_{15}W}$: C, 21.26; H, 1.67; N, 0.64. Found: C, 21.88; H, 1.54; N, 0.89.

To an acetonitrile (20 mL) solution of **1** (60 mg, 48 μmol) was added an acetonitrile (10 mL) solution of $[\mathrm{TTF}]_3[\mathrm{BF_4}]_2$ (40 mg, 48 μmol), and the solution was stirred for 2 h at room temperature. The product $[\mathrm{NBu^n_4}]_{0.2}[\mathrm{W(C_3S_5)_3}]$ (**7**) was collected by centrifugation, washed with acetonitrile and diethyl ether, and dried in vacuo (55% yield). Anal. Calcd for $\mathrm{C_{12.2}H_{7.2}N_{0.2}S_{15}W}$: C, 18.28; H, 0.98; N, 0.34. Found: C, 17.84; H, 0.88; N, 0.34.

By a similar procedure, complex **2** reacted with an excess amount of iodine in acetonitrile to afford $[\mathrm{NBu^n_4}]_{0.3}[\mathrm{Mo(C_3S_5)_3}]$ (**8**) (76% yield), as described previously.[14] A reaction of **2** with an excess amount of $[\mathrm{Fe(C_5H_5)_2}][\mathrm{PF_6}]$ in acetonitrile afforded a black precipitate of $[\mathrm{NBu^n_4}]_{0.4}[\mathrm{Mo(C_3S_5)_3}]$ (**9**) (44% yield). Anal. Calcd for $\mathrm{C_{15.4}H_{14.4}N_{0.4}S_{15}Mo}$: C, 23.65; H, 1.85; N, 0.71. Found: C, 23.14; H, 1.71; N, 0.89. A reaction of **2** with an excess amount of $[\mathrm{TTF}]_3[\mathrm{BF_4}]_2$ in acetonitrile gave $[\mathrm{NBu^n_4}]_{0.05}[\mathrm{Mo(C_3S_5)_3}]$ (**10**) (63% yield), as described previously.[14]

Preparations of $[\mathrm{NBu^n_4}]_{0.8}[\mathrm{W(C_3S_5)_3}]$ (11) and $[\mathrm{NBu^n_4}]_{0.3}[\mathrm{W(C_3S_5)_3}]$ (12) by Electro-oxidation. A dichloromethane (50 mL) solution containing both **1** (31 mg, 1.0 mmol) and $[\mathrm{NBu^n_4}][\mathrm{ClO_4}]$ (1.71 g, 200 mmol) was subjected to a controlled-current (1 mA) electrolysis for 40 min under a nitrogen atmosphere in a cell consisting of platinum wires (anode and cathode). After the concentration of the resulting solution, addition of methanol afforded a black precipitate of **11**, which was collected by centrifugation, washed with methanol and diethyl ether, and dried in vacuo (30% yield). Anal. Calcd for $\mathrm{C_{21.8}H_{28.8}N_{0.8}S_{15}W}$: C, 26.91; H, 3.00; N, 1.96. Found: C, 26.91; H, 3.00; N, 1.20.

Similarly, the electrolysis of **1** (31 mg, 1.0 mmol) in the presence of $[\mathrm{NBu^n_4}][\mathrm{ClO_4}]$ (1.71 g, 200 mmol) in acetonitrile (50 mL) was performed to give black microcrystals of **12** on the anode. They were washed with methanol and diethyl ether and dried in vacuo (34% yield). Anal. Calcd for $\mathrm{C_{13.8}H_{10.8}N_{0.3}S_{15}W}$: C, 19.84; H, 1.29; N, 0.50. Found: C, 19.84; H, 1.39; N, 0.59.

Measurements. Electronic absorption spectra were measured as described previously.[18] IR spectra were measured on a Perkin-Elmer 983G spectrophotometer for KBr disks. ESR spectra were recorded on JEOL ME-2X and JES-FEIX spectrometers and calibrated with signals of $\mathrm{MnO_2}$. Electrical resistivities of the complexes were measured for compacted pellets by the conventional two-probe method.[19] Cyclic voltammograms of complexes **1** and **2** were recorded in dimethylformamide and dichloromethane using $[\mathrm{NBu^n_4}][\mathrm{ClO_4}]$ as an electrolyte, as described previously.[20] Magnetic susceptibilities of **3** and **4** at room temperature were determined by using a Gouy magnetic apparatus. Magnetic susceptibilities of **3** over the range of liquid-helium temperature to room temperature were measured by the Faraday method. The instrument was calibrated with $\mathrm{CuSO_4{\cdot}5H_2O}$.

Theoretical Calculations of $\mathrm{C_3S_5}^{2-}$ and $\mathrm{C_3S_5}^{-}$ Moieties. Semi-empirical PM3 calculations of these ligand moieties were carried out by use of MOPAC version 6.02 on an NEC SX-3/Model 14R computer at the Computation Center, Osaka University.[21] The eigenvector-following routine was adopted as the geometry optimization algorithm for both the cases, and the UHF option was used for the calculation of $\mathrm{C_3S_5}^{-}$.

Table I. Crystallographic Data for $[\mathrm{NBu^n_4}]_2[\mathrm{W(C_3S_5)_3}]$ (1), $[\mathrm{NBu^n_4}]_2[\mathrm{Mo(C_3S_5)_3}]$ (2), and $[\mathrm{Fe(C_5Me_5)_2}][\mathrm{W(C_3S_5)_3}]$ (3)

	1	2	3
chem formula	$\mathrm{C_{41}H_{72}N_2S_{15}W}$	$\mathrm{C_{41}H_{72}MoN_2S_{15}}$	$\mathrm{C_{29}H_{30}FeS_{15}W}$
fw	1257.87	1169.96	1099.24
space group	$Pca2_1$ (No. 29)	$Pca2_1$ (No. 29)	$P\bar{1}$ (No. 2)
a, Å	32.905(7)	32.881(13)	12.150(2)
b, Å	10.778(2)	10.788(5)	14.756(1)
c, Å	16.398(3)	16.382(9)	11.9041(9)
α, deg	90.0	90.0	110.771(6)
β, deg	90.0	90.0	97.087(8)
γ, deg	90.0	90.0	83.84(1)
V, Å^3	5816(2)	5811(5)	1975.7(4)
Z	4	4	2
ρ_c, g cm^{-3}	1.436	1.337	1.848
T, °C	23	23	23
μ, cm^{-1}	26.5	7.68	42.4
no. of unique data used ($\lvert F_o\rvert > 3\sigma(F)$)	4847	3303	9578
$R(F_o)^a$	0.080	0.087	0.040
$R_w(F_o)^b$	0.099		0.044

[a] $R(F_o) = \sum\lvert\lvert F_o\rvert - \lvert F_c\rvert\rvert/\sum\lvert F_o\rvert$. [b] $R_w(F_o) = [\sum w(\lvert F_o\rvert - \lvert F_c\rvert)^2/\sum w\lvert F_o\rvert^2]^{1/2}$.

X-ray Crystal Structure Determinations of $[\mathrm{NBu^n_4}]_2[\mathrm{W(C_3S_5)_3}]$ (1), $[\mathrm{NBu^n_4}]_2[\mathrm{Mo(C_3S_5)_3}]$ (2), and $[\mathrm{Fe(C_5Me_5)_2}][\mathrm{W(C_3S_5)_3}]$ (3). Diffraction data were obtained on a Rigaku AFC-5R four-circle diffractometer at the Faculty of Science, Osaka University, using graphite-monochromated Mo Kα (λ = 0.710 69 Å) radiation. Crystal data and details of measurements for complexes **1**–**3** are summarized in Table I (see supplementary material for data collection parameters). Three standard reflections were monitored after every 100 reflections. No significant decays in their intensities were observed throughout the data collection. Reflection data were corrected for Lorentz and polarization effects as well as absorption.[22]

The structures were solved by direct methods[23] and refined by the full-matrix least-squares technique. All the non-hydrogen atoms of complex **3** were refined anisotropically. However, for complexes **1** and **2** the anion moieties were refined anisotropically and the cations isotropically and some of methyl carbons of the tetrabutylammonium groups were not found from difference Fourier syntheses owing to their large temperature factors and omitted from the subsequent calculations. The calculations were performed with the TEXSAN structure analysis package[24] on a VAX-II computer at the Faculty of Science, Osaka University, and with SHELX 76[25] on an ACOS S930 computer at the Research Center for Protein Engineering, Institute for Protein Research, Osaka University. Atomic scattering factors were taken from the usual sources.[26] The final positional and thermal parameters for non-hydrogen atoms for **1**–**3** are given in Tables II–IV, respectively. Figures 5, 6, and 8 were drawn with a local version of ORTEP II.[27]

Results and Discussion

Electrochemical and Spectroscopic Properties of Complexes 1 and 2. Figure 1 shows cyclic voltammograms of **1** and **2** in

---

(17) Matsubayashi, G.; Nojo, T.; Tanaka, T. *Inorg. Chim. Acta* **1988**, *154*, 133.

(18) Matsubayashi, G.; Tanaka, S.; Yokozawa, A. *J. Chem. Soc., Dalton Trans.* **1992**, 1827.

(19) Ueyama, K.; Matsubayashi, G.; Tanaka, T. *Inorg. Chim. Acta* **1984**, *87*, 143.

(20) Tanaka, S.; Matsubayashi, G. *J. Chem. Soc., Dalton Trans.* **1992**, 2837.

(21) MOPAC version 6 coded by: Stewart, J. J. P. *QCPE Bull.* **1989**, *9*, 10. Revised as version 6.02 for the NEC SX-2N machine by: Takagi, T.; Matsumura, K.; Noda, A.; Onozawa, N.; Fujiwara, H. *Bull. Computation Center Osaka Univ.* **1992**, *22*, 1.

(22) North, A. C. T.; Phillips, D. C.; Matheus, F. C. *Acta Crystallogr.* **1968**, *A24*, 351.

(23) Gilmore, C. J. MITHRIL: an integrated direct methods computer program. *J. Appl. Crystallogr.* **1984**, *17*, 42. Beurskens, P. T. DIRDIF: direct methods for difference structures-an automatic procedure for phase extension and refinement of difference structure factors, Technical Report 1984/1, Crystallography Laboratory, Toernooiveld, Nijmegen, 1984.

(24) TEXSAN: Structure Analysis Package, Molecular Structure Corp., College Station, TX, 1985.

(25) Sheldrick, G. M. SHELX 76, a Computer Program for Crystal Structure Determination, University of Cambridge, 1976.

(26) *International Tables for X-Ray Crystallography*; Kynoch Press: Birmingham, England, 1974; Vol. IV.

(27) Johnson, C. K. ORTEP-II, Report ORNL 5138, Oak Ridge National Laboratory, Oak Ridge, TN, 1976.

Table II. Atomic Coordinates and Equivalent Isotropic Thermal Parameters (Å^2) for Non-Hydrogen Atoms of $[NBu^n_4]_2[W(C_3S_5)_3]$ (**1**)[a]

atom	*x*	*y*	*z*	*B*(eq)[b]
W	0.10786(2)	0.01419(7)	0.5	3.65(1)
S(1)	0.1700(2)	0.0536(7)	0.4297(5)	5.0(1)
S(2)	0.2070(3)	0.2621(8)	0.3324(6)	7.0(1)
S(3)	0.2062(6)	0.5195(11)	0.2639(12)	10.8(1)
S(4)	0.1353(3)	0.4113(7)	0.3469(5)	6.4(1)
S(5)	0.0901(2)	0.2095(5)	0.4393(4)	4.5(1)
S(6)	0.0875(2)	0.1183(6)	0.6223(3)	4.6(1)
S(7)	0.1127(3)	0.1156(10)	0.7995(4)	7.1(1)
S(8)	0.1570(6)	0.0168(15)	0.9417(4)	13.2(1)
S(9)	0.1722(3)	−0.0751(11)	0.7730(4)	7.1(1)
S(10)	0.1511(2)	−0.0941(6)	0.5929(4)	4.8(1)
S(11)	0.0362(1)	−0.0180(5)	0.4876(5)	4.5(1)
S(12)	−0.0182(2)	−0.2048(7)	0.4033(5)	6.5(1)
S(13)	−0.0333(4)	−0.4368(12)	0.3079(9)	12.2(1)
S(14)	0.0493(2)	−0.3551(7)	0.3512(5)	6.6(1)
S(15)	0.1107(2)	−0.1789(6)	0.4272(4)	4.7(1)
C(1)	0.1664(5)	0.1981(13)	0.3847(11)	5.2(2)
C(2)	0.1832(5)	0.3982(14)	0.3050(16)	6.5(2)
C(3)	0.1327(5)	0.2654(14)	0.3901(14)	4.7(2)
C(4)	0.1172(5)	0.0625(18)	0.7008(6)	4.9(2)
C(5)	0.1475(8)	0.0171(23)	0.8429(6)	6.8(2)
C(6)	0.1455(6)	−0.0245(19)	0.6878(6)	4.9(2)
C(7)	0.0295(4)	−0.1521(15)	0.4310(13)	5.3(2)
C(8)	−0.0026(3)	−0.3380(14)	0.3538(12)	6.3(2)
C(9)	0.0611(4)	−0.2228(13)	0.4060(12)	4.7(2)
N(1)	0.4285(7)	0.0283(19)	0.6757(14)	8.2(3)
C(11)	0.4553(8)	0.0530(28)	0.7481(17)	8.1(3)
C(12)	0.4971(9)	0.1065(30)	0.7227(19)	9.5(3)
C(13)	0.5237(10)	0.1390(30)	0.7975(20)	10.2(3)
C(14)	0.5617(12)	0.2019(34)	0.7752(26)	12.4(4)
C(15)	0.4199(11)	0.1389(23)	0.6217(19)	8.9(3)
C(16)	0.4011(15)	0.2554(28)	0.6628(23)	13.0(4)
C(17)	0.4031(16)	0.3604(34)	0.5974(26)	13.2(4)
C(19)	0.3932(9)	−0.0220(29)	0.7230(22)	9.2(4)
C(20)	0.3599(11)	−0.0699(34)	0.6643(24)	11.5(4)
C(21)	0.3229(13)	−0.1273(38)	0.7111(28)	15.0(4)
C(22)	0.2842(15)	−0.1771(38)	0.6769(31)	15.2(4)
C(23)	0.4468(11)	−0.0619(24)	0.6164(18)	9.1(3)
C(24)	0.4521(14)	−0.1889(28)	0.6601(24)	12.6(4)
C(25)	0.4702(16)	−0.2827(38)	0.5971(27)	15.9(4)
C(26)	0.4533(18)	−0.3120(41)	0.5166(31)	18.5(4)
N(2)	0.1750(8)	0.4831(22)	0.6203(18)	8.8(3)
C(31)	0.1318(8)	0.4507(27)	0.5953(23)	9.1(3)
C(32)	0.0984(9)	0.5493(28)	0.6079(23)	8.7(3)
C(33)	0.0598(10)	0.5092(27)	0.5616(27)	10.0(4)
C(34)	0.0277(11)	0.5960(30)	0.5847(25)	10.7(4)
C(35)	0.2002(17)	0.3700(33)	0.6455(26)	17.8(4)
C(36)	0.2093(17)	0.2862(37)	0.5714(27)	14.5(4)
C(37)	0.1924(14)	0.5836(32)	0.5647(25)	12.1(4)
C(38)	0.1667(25)	0.5340(41)	0.7063(22)	19.1(4)

[a] Estimated standard deviations in parentheses. [b] *B*(eq) is the isotropic equivalent of the anisotropic thermal parameter.

dimethylformamide. Both the complexes exhibit two almost reversible redox waves due to the $[M(C_3S_5)_3]^{2-/-}$ and $[M(C_3S_5)_3]^{-/0}$ couples at $E_{1/2}{}^{\circ}$ = 0.145 and 0.325 (M = W)[28] and 0.185 and 0.38 V (vs SCE) (M = Mo), respectively. These findings are similar to those for the $[Mo(S_2C_2(CF_3)_2)_3]^{2-}$,[29] $[Mo(S_2C_2(COOMe)_2)_3]^{2-}$,[30] and $[M(S_2C_2S_2CO)_3]^{2-}$ (M = W, Mo) complexes.[28] The redox potentials for the present tungsten complex in dimethylformamide, which are somewhat smaller than those of the molybdenum analog, appear at further low energies ($E_{1/2}{}^{\circ}$ = +0.03 and +0.275 V vs SCE) in dichloromethane.

Electronic absorption spectra of **1** in acetonitrile in the presence of varying amounts of $[Fe(C_5H_5)_2][PF_6]$ are illustrated in Figure 2. By the addition of some amounts of $[Fe(C_5H_5)_2][PF_6]$ as an oxidant to the solution of **1** successively to an equimolar amount of **1**, the spectrum of **1** is changed with the generation of some isosbestic points, resulting in the spectrum of the one-electron-oxidized $[W(C_3S_5)_3]^-$ complex. Further addition of $[Fe(C_5H_5)_2][PF_6]$ to the solution exhibits spectral changes with alternate isosbestic points to give the final spectrum of the $[W(C_3S_5)_3]^0$ species. A similar spectral change is observed for the molybdenum analog **2** in the presence of the $[Fe(C_5H_5)_2]^+$ cation.[14] The ligand π–π^* transition bands[31] which occur at 500 and 490 nm for **1** and **2**, respectively, are shifted to 430 and 410 nm for the oxidized $[W(C_3S_5)_3]^-$ and $[Mo(C_3S_5)_3]^-$ species. Furthermore, these oxidized species exhibit characteristic intense bands at 680 and 750 nm, respectively. These bands are close to the band observed

Table III. Atomic Coordinates and Equivalent Isotropic Thermal Parameters (Å^2) for Non-Hydrogen Atoms of $[NBu^n_4]_2[Mo(C_3S_5)_3]$ (**2**)[a]

atom	*x*	*y*	*z*	*B*(eq)[b]
Mo	0.10785(6)	0.0136(2)	0.5	3.81(4)
S(1)	0.1710(2)	0.0537(8)	0.4317(5)	5.5(2)
S(2)	0.2079(3)	0.2632(9)	0.3348(6)	7.7(3)
S(3)	0.2047(5)	0.5190(12)	0.2606(10)	12.1(5)
S(4)	0.1354(3)	0.4107(8)	0.3479(6)	6.7(3)
S(5)	0.0899(2)	0.2098(7)	0.4385(5)	4.7(1)
S(6)	0.0882(2)	0.1213(7)	0.6230(4)	4.8(2)
S(7)	0.1138(3)	0.1174(10)	0.8009(5)	7.2(2)
S(8)	0.1601(5)	0.0244(22)	0.9406(7)	16.1(8)
S(9)	0.1721(3)	−0.0744(11)	0.7733(5)	7.2(3)
S(10)	0.1511(2)	−0.0948(8)	0.5951(4)	5.1(2)
S(11)	0.0364(2)	−0.0195(6)	0.4880(5)	4.7(1)
S(12)	−0.0182(2)	−0.2070(8)	0.4041(6)	6.5(2)
S(13)	−0.0334(4)	−0.4365(13)	0.3076(9)	13.0(4)
S(14)	0.0495(3)	−0.3552(7)	0.3515(5)	6.5(2)
S(15)	0.1107(2)	−0.1801(6)	0.4272(5)	4.9(2)
C(1)	0.1676(6)	0.1988(17)	0.3865(16)	5.6(8)
C(2)	0.1846(7)	0.4012(19)	0.3123(21)	8.6(13)
C(3)	0.1328(6)	0.2655(17)	0.3898(14)	5.5(8)
C(4)	0.1179(7)	0.0655(21)	0.7019(9)	4.6(7)
C(5)	0.1478(9)	0.0163(28)	0.8431(10)	7.5(11)
C(6)	0.1453(7)	−0.0260(20)	0.6900(9)	5.0(7)
C(7)	0.0293(5)	−0.1567(18)	0.4338(15)	4.6(7)
C(8)	−0.0022(5)	−0.3382(22)	0.3533(18)	8.7(13)
C(9)	0.0610(5)	−0.2230(18)	0.4060(16)	4.9(7)
N(1)	0.4291(6)	0.0289(21)	0.6765(14)	8.4(7)
C(11)	0.4575(7)	0.0588(26)	0.7430(15)	8.3(8)
C(12)	0.4980(8)	0.1217(31)	0.7225(17)	8.3(9)
C(13)	0.5221(8)	0.1447(34)	0.8015(19)	9.2(9)
C(14)	0.5604(9)	0.2080(38)	0.7817(24)	11.1(12)
C(15)	0.4204(9)	0.1390(21)	0.6252(16)	8.1(8)
C(16)	0.4040(13)	0.2552(30)	0.6666(22)	12.3(13)
C(17)	0.4058(13)	0.3641(29)	0.6053(27)	13.1(14)
C(18)	0.3743(17)	0.4566(42)	0.6251(39)	19.7(25)
C(19)	0.3908(7)	−0.0183(32)	0.7145(19)	11.5(12)
C(20)	0.3566(10)	−0.0739(38)	0.6620(21)	10.6(12)
C(21)	0.3240(11)	−0.1354(42)	0.7151(23)	12.7(14)
C(22)	0.2895(11)	−0.1784(46)	0.6653(30)	14.6(16)
C(23)	0.4460(9)	−0.0682(23)	0.6207(17)	9.3(9)
C(24)	0.4518(12)	−0.1941(31)	0.6591(21)	10.6(11)
C(25)	0.4763(13)	−0.2770(36)	0.6015(32)	16.9(20)
C(26)	0.4550(15)	−0.2988(50)	0.5243(27)	16.4(19)
N(2)	0.1760(6)	0.4685(22)	0.6233(14)	8.9(7)
C(31)	0.1333(6)	0.4437(27)	0.5976(20)	8.9(9)
C(32)	0.1001(8)	0.5443(30)	0.6094(22)	9.6(10)
C(33)	0.0608(8)	0.5110(30)	0.5669(20)	8.6(8)
C(34)	0.0286(8)	0.6035(33)	0.5873(24)	9.8(10)
C(35)	0.2029(10)	0.3537(30)	0.6121(27)	13.6(15)
C(39)	0.1929(11)	0.5681(32)	0.5713(22)	13.0(14)
C(40)	0.2323(12)	0.6170(58)	0.5397(36)	24.5(33)
C(41)	0.2267(12)	0.7067(42)	0.4686(25)	14.0(15)
C(42)	0.2642(16)	0.7723(53)	0.4510(39)	22.5(28)
C(43)	0.1765(13)	0.5065(41)	0.7096(16)	16.6(19)
C(44)	0.1617(21)	0.4543(46)	0.7907(29)	21.1(26)
C(45)	0.1628(18)	0.5475(55)	0.8603(22)	17.7(21)

[a] Estimated standard deviations in parentheses. [b] *B*(eq) is the isotropic equivalent of the anisotropic thermal parameter.

---

(28) $E_{1/2}{}^{\circ}$ values +0.01 and +0.31 V (vs Ag/AgCl) were reported for the $[W(C_3S_5)_3]^{2-/-}$ and $[W(C_3S_5)_3]^{-/0}$ processes: Yang, X.; Freeman, G. K. W.; Rauchfuss, T. B.; Wilson, S. R. *Inorg. Chem.* **1991**, *30*, 3034.

(29) Wharton, E. J.; McCleverty, J. A. *J. Chem. Soc. A* **1969**, 2258.

(30) Draganjac, M.; Coucouvanis, D. *J. Am. Chem. Soc.* **1983**, *105*, 139.

(31) Matsubayashi, G.; Takahashi, K.; Tanaka, T. *J. Chem. Soc., Dalton Trans.* **1988**, 967.

Table IV. Atomic Coordinates and Isotropic Thermal Parameters (Å^2) for Non-Hydrogen Atoms of $[Fe(C_5Me_5)_2][W(C_3S_5)_3]$ (**3**)[a]

atom	*x*	*y*	*z*	*B*(eq)[b]
W	0.37855(1)	0.20939(1)	−0.06521(2)	1.253(3)
Fe	0.20046(5)	0.70855(5)	0.39040(6)	1.27(1)
S(1)	0.2083(1)	0.25514(9)	0.0244(1)	2.30(2)
S(2)	0.0612(1)	0.16505(9)	0.1340(1)	2.14(2)
S(3)	−0.0057(1)	0.0048(1)	0.2010(2)	2.80(3)
S(4)	0.1937(1)	−0.01611(9)	0.0699(1)	2.57(2)
S(5)	0.3494(1)	0.05502(9)	−0.0575(1)	2.77(2)
S(6)	0.2938(1)	0.3124(1)	−0.1710(1)	2.65(3)
S(7)	0.2741(2)	0.3136(2)	−0.4257(2)	2.16(4)
S(8)	0.3340(3)	0.2767(3)	−0.6779(2)	3.07(6)
S(9)	0.4065(2)	0.1302(2)	−0.5077(1)	2.49(3)
S(10)	0.4363(1)	0.1147(1)	−0.2588(1)	2.22(2)
S(11)	0.5653(1)	0.16385(9)	−0.0063(1)	1.87(2)
S(12)	0.7702(1)	0.2784(1)	0.0927(1)	1.63(2)
S(13)	0.8845(1)	0.4609(1)	0.2162(2)	2.41(4)
S(14)	0.6392(1)	0.4598(1)	0.1750(2)	2.38(3)
S(15)	0.4237(1)	0.3625(1)	0.0813(2)	2.36(3)
C(1)	0.1767(4)	0.1590(3)	0.0588(4)	1.41(7)
C(2)	0.0790(4)	0.0492(3)	0.1383(5)	1.90(8)
C(3)	0.2385(4)	0.0736(3)	0.0258(4)	1.58(7)
C(4)	0.3188(5)	0.2586(4)	−0.3180(5)	1.60(10)
C(5)	0.3386(7)	0.2264(7)	−0.5437(7)	1.90(15)
C(6)	0.3787(5)	0.1750(5)	−0.3561(5)	1.57(10)
C(7)	0.6268(4)	0.2717(3)	0.0643(4)	1.24(7)
C(8)	0.7707(4)	0.4031(4)	0.1638(5)	1.62(10)
C(9)	0.5654(4)	0.3567(3)	0.1023(5)	1.49(8)
C(11)	0.1107(4)	0.5941(4)	0.3876(6)	2.30(11)
C(12)	0.1141(4)	0.5916(4)	0.2695(6)	2.23(11)
C(13)	0.0627(4)	0.6808(4)	0.2597(5)	1.47(9)
C(14)	0.0279(4)	0.7383(3)	0.3740(5)	1.80(9)
C(15)	0.0566(4)	0.6860(4)	0.4551(5)	2.01(9)
C(16)	0.1502(7)	0.5131(5)	0.4349(10)	4.91(25)
C(17)	0.1593(6)	0.5069(5)	0.1668(8)	3.93(18)
C(18)	0.0448(6)	0.7100(7)	0.1498(7)	1.87(14)
C(19)	−0.0341(5)	0.8369(5)	0.4051(8)	3.43(16)
C(20)	0.0321(6)	0.7190(6)	0.5848(6)	2.77(13)
C(21)	0.3260(5)	0.7602(5)	0.5301(5)	1.45(10)
C(22)	0.3715(4)	0.6830(5)	0.4319(6)	1.74(11)
C(23)	0.3532(4)	0.7142(4)	0.3297(5)	1.59(8)
C(24)	0.2967(4)	0.8091(4)	0.3658(5)	1.64(8)
C(25)	0.2798(5)	0.8371(4)	0.4876(5)	1.95(10)
C(26)	0.3300(8)	0.7651(9)	0.6584(7)	2.32(19)
C(27)	0.4306(6)	0.5876(6)	0.4317(9)	3.74(22)
C(28)	0.3884(5)	0.6587(4)	0.2058(6)	2.60(11)
C(29)	0.2661(5)	0.8682(5)	0.2849(7)	2.94(15)
C(30)	0.2261(7)	0.9329(5)	0.5617(8)	4.11(18)

[a] Estimated standard deviations in parentheses. [b] *B*(eq) is the isotropic equivalent of the anisotropic thermal parameter.

for the isoelectronic $[Re(C_3S_5)_3]^0$ species[13] and are likely ascribed to metal-to-ligand charge-transfer bands.[32] These bands are intensified for the further oxidized $[W(C_3S_5)_3]^0$ and $[Mo(C_3S_5)_3]^0$ species.

Complexes **1** and **2** show the IR C=C stretching band of the C_3S_5 ligand at 1440 cm^{-1}. For the one-electron-oxidized species **3**, **4**, and **11** the bands occur at 1380, 1360, and 1380 cm^{-1}, respectively. Essentially two-electron-oxidized species **5**, **7**, and **10** afford the bands at 1330, 1330, and 1310 cm^{-1}, respectively. Partially oxidized complexes **7**–**9** and **12** exhibit the C=C stretching bands corresponding to both one- and two-electron-oxidized species. These low-frequency shifts of the C=C stretching band upon the oxidation of the $[M(C_3S_5)_3]^{2-}$ anions were also observed for other C_3S_5–metal complexes.[8,13,33]

Figure 3 shows powder ESR spectra of **3** and **5**. Although complexes **1** and **2** are diamagnetic, **3** and **4** contain both the paramagnetic cation and anion species, and the broad signals around g = 2.0 seem to be due to the $[W(C_3S_5)_3]^-$ and $[Mo(C_3S_5)_3]^-$ anions, while the signals of the decamethylferrocenium cation derivatives are difficult to detect.[8,34] The signal broadening (the peak-to-peak line width is 90 mT for **3** and **4**) is likely caused by some molecular interactions among the

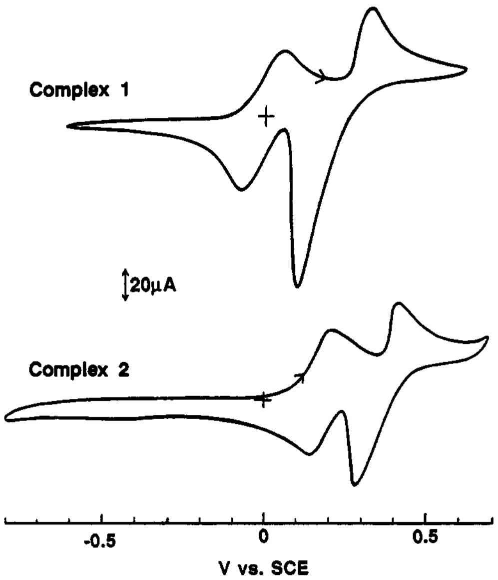

Figure 1. Cyclic voltammograms of **1** (1.0 × 10^{-4} mol L^{-1}) and **2** (1.0 × 10^{-4} mol L^{-1}) in dimethylformamide at room temperature, referenced to SCE (0.1 mol L^{-1} $[NBu^n_4][ClO_4]$, sweep rate 0.1 V s^{-1}).

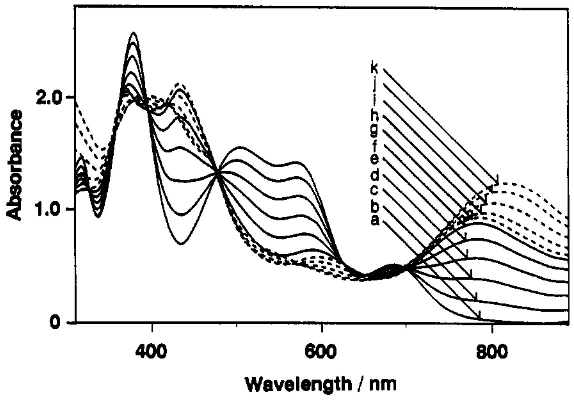

Figure 2. Electronic absorption spectra of **1** (8.0 × 10^{-5} mol L^{-1}) in acetonitrile in the presence of $[Fe(C_5H_5)_2][PF_6]$. Concentration (mol L^{-1}): (a) 0; (b) 1.6 × 10^{-5}; (c) 3.2 × 10^{-5}; (d) 4.8 × 10^{-5}; (e) 6.4 × 10^{-5}; (f) 8.0 × 10^{-5}; (g) 9.5 × 10^{-5}; (h) 1.1 × 10^{-4}; (i) 1.3 × 10^{-4}; (j) 1.4 × 10^{-4}; (k) 1.6 × 10^{-4}.

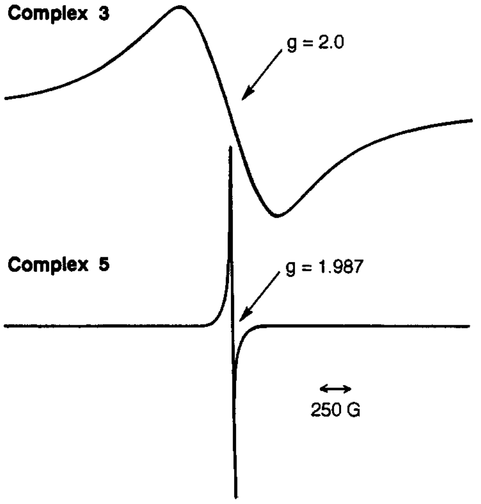

Figure 3. Powder ESR spectra of **3** and **5** at room temperature.

---

(32) Schrauzer, G. N.; Mayweg, V. P. *J. Am. Chem. Soc.* **1966**, *88*, 3235.

(33) Sakamoto, Y.; Matsubayashi, G.; Tanaka, T. *Inorg. Chim. Acta* **1986**, *113*, 137.

(34) Horsfield, A.; Wassermann, A. *J. Chem. Soc. A* **1970**, 3202.

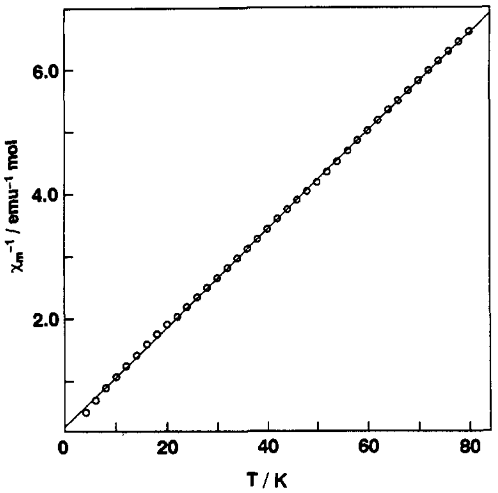

Figure 4. Temperature dependence of the magnetic susceptibility of 3.

paramagnetic anions. It is confirmed from the crystal structure determination for 3, as described below. Sharp signals of the anions (g = 1.988 and 2.008 for 3 and 4; line width = 6.0 mT) have occurred in dichloromethane at room temperature. For complex 5 a sharp powder ESR signal (g = 1.987; line width = 1.5 mT) is observed. This complex is an almost two-electron-oxidized species, containing a small amount of the paramagnetic $[W(C_3S_5)_3]^-$ anion. The anion moieties are surrounded by the diamagnetic $[W(C_3S_5)_3]^0$ species, which is similar to the situation of the $[W(C_3S_5)_3]^-$ anion in solution. Similarly, 6–9, 10, and 12 also exhibit a rather sharp ESR signal, which is ascribed to the $[W(C_3S_5)_3]^-$ or the $[Mo(C_3S_5)_3]^-$ species. These salts contain small amounts of these paramagnetic species, which are isolated by surrounding diamagnetic $[W(C_3S_5)_3]^0$ and $[Mo(C_3S_5)_3]^0$ moieties.

Magnetic susceptibilities for complexes 3 and 4 have been measured. The susceptibilities of $+3720 \times 10^{-6}$ and $+3710 \times 10^{-6}$ emu mol^{-1} (effective magnetic moments, 3.17 and 3.12 μ_B) at room temperature for 3 and 4, respectively, almost correspond to the sum of susceptibilities of the paramagnetic cation and anion for these complexes. The magnetic susceptibility of 3 was measured over the temperature range 4.2–300 K. Figure 4 illustrates the temperature dependence of the susceptibility in the low-temperature region. The susceptibility obeys essentially the Curie law in this temperature region, indicating no appreciable magnetic interaction among paramagnetic cations and/or anions in the solid state.

Crystal Structures of 1 and 2. Both complexes are isomorphous and have essentially the same crystal structure consisting of discrete anions and cations without any significant close atom–atom contacts among them. A perspective view of the anion moiety of 1 is illustrated in Figure 5, together with the atom-labeling scheme. Bond distances and angles relevant to the tungsten and molybdenum coordination spheres of 1 and 2 are listed in Table V. The structure of the anion in 1 shows three C_3S_5 ligands coordinated to the tungsten atom. The S_3 (coordinated sulfur atoms) triangles are twisted with respect to each other by an average of 16°. Since the twist angle (ϕ) is 0° in the trigonal prism and 60° in the octahedron, the geometry of the present complex is rather close to that of a trigonal prism. This geometry is very close to that of 2 (average ϕ = 11°). In accordance with these angles, the interligand transoid S–M–S angles are 146.5 and 147.2° for 1 and 2, respectively, with the limiting angles of 136 and 180° for a trigonal prism and perfect octahedron. They are somewhat different from the intermediate geometry between the octahedron and the trigonal prism observed for $[M(S_2C_2(CN)_2)_3]^{2-}$ (M = W, Mo) (ϕ = 28°)[35] and

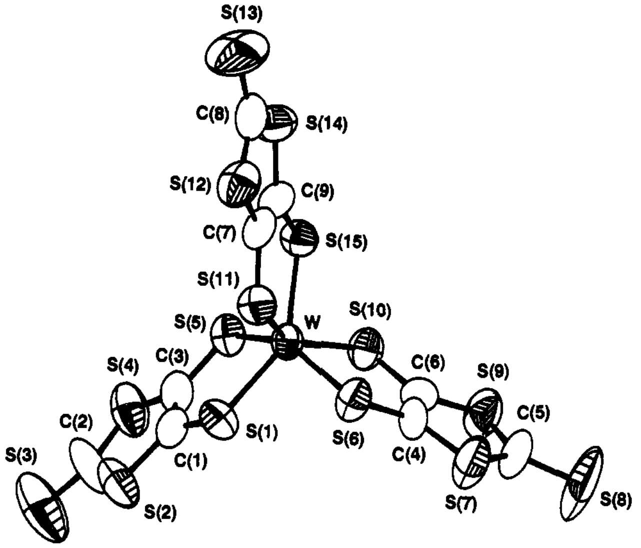

Figure 5. Geometry of the anion moiety of 1 together with the atom-labeling scheme.

Table V. Bond Distances (Å) and Angles (deg) Relevant to the Metal Coordination Spheres of $[NBu^n{}_4]_2[W(C_3S_5)_3]$ (**1**) and $[NBu^n{}_4]_2[Mo(C_3S_5)_3]$ (**2**)

	1 (M = W)	**2** (M = Mo)
M–S(1)	2.385(4)	2.398(8)
M–S(5)	2.401(4)	2.408(8)
M–S(6)	2.391(4)	2.414(7)
M–S(10)	2.394(4)	2.412(8)
M–S(11)	2.402(4)	2.385(7)
M–S(15)	2.391(4)	2.408(7)
S(1)–M–S(5)	81.5(2)	81.9(3)
S(1)–M–S(6)	124.1(2)	122.2(3)
S(1)–M–S(10)	83.3(2)	83.0(3)
S(1)–M–S(11)	146.1(2)	147.4(3)
S(1)–M–S(15)	83.1(2)	83.8(3)
S(5)–M–S(6)	82.4(2)	82.1(3)
S(5)–M–S(10)	146.9(2)	147.0(3)
S(5)–M–S(11)	81.5(2)	81.7(3)
S(5)–M–S(15)	124.3(2)	124.2(3)
S(6)–M–S(10)	82.0(2)	81.4(3)
S(6)–M–S(11)	82.2(2)	83.0(3)
S(6)–M–S(15)	146.5(2)	147.3(3)
S(10)–M–S(11)	124.8(2)	124.1(3)
S(10)–M–S(15)	82.5(2)	82.9(3)
S(11)–M–S(15)	82.6(2)	82.4(2)

$[W(S_2C_2S_2CO)_3]^{2-}$ complexes (transoid S–W–S angle = 153.1°)[28] and from the essentially trigonal prismatic geometry for the $[Mo(S_2C_2(COOMe)_2)_3]^{2-}$ complex (transoid S–Mo–S angle = 135°).[30] Bidentate dithiolene ligands, S(1)–S(5), S(6)–S(10), and S(11)–S(15), are almost planar with displacements from the best planes of ±0.06, ±0.06, and ±0.02 Å, respectively. The metal atom also lies essentially on these planes. The average W–S distance (2.394 Å) is close to those for $[PPh_4]_2[W(S_2C_2S_2CO)_3]$ (average 2.394 Å)[28] and for $[AsPh_4]_2[W(S_2C_2(CN)_2)_3]$ (average 2.371 Å).[35] The average Mo–S distance (2.404 Å) for 2 is also close to 2.373 Å for $[AsPh_4]_2[Mo(S_2C_2(CN)_2)_3]$[35] and 2.393 Å for $[PPh_4]_2[Mo(S_2C_2(COOMe)_2)_3]$.[30]

Crystal Structure of 3. Geometries of the cation and the anion of 3 are displayed in Figure 6, together with the atom-labeling scheme. Selected bond distances and angles are summarized in Table VI. The C_5 rings of the C_5Me_5 moieties are rotated by 21.5° away from the ideal D_{5h} symmetry. This geometry is very close to that of one of the cations of $[Fe(C_5Me_5)_2][Fe(C_3S_5)_2]$ (21.6° twist angle)[20] and rather close to those of essentially staggered forms (36° twist angle) observed for $[Fe(C_5Me_5)_2]^+$

---

[35] Brown, G.; Stiefel, E. I. *Inorg. Chem.* **1973**, *12*, 2140.

[36] Miller, J. S.; Calabrese, J. C.; Rommelmann, H.; Chittipeddi, S. R.; Reiff, W. M.; Epstein, A. J. *J. Am. Chem. Soc.* **1987**, *109*, 769.

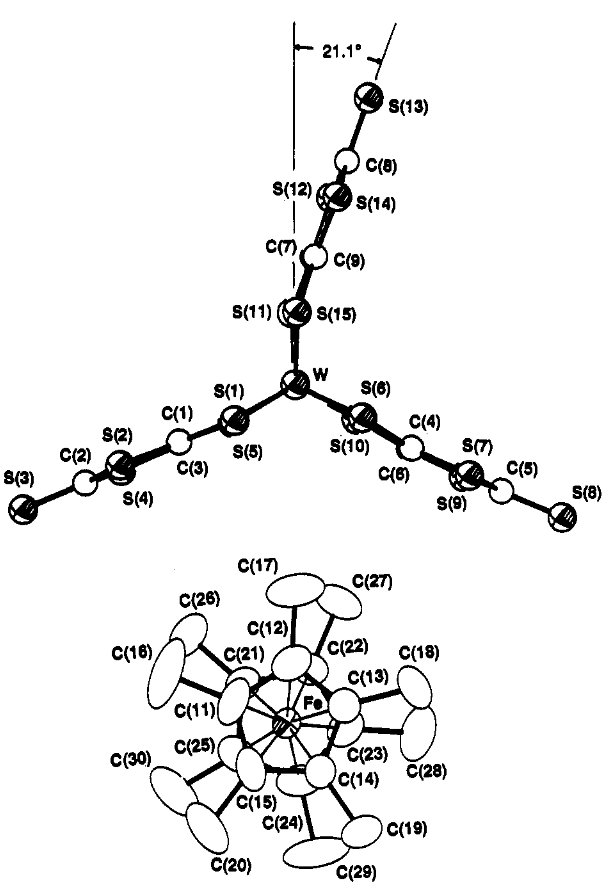

Figure 6. Geometries of the cation and the anion of **3** together with the atom-labeling scheme.

Table VI. Selected Bond Distances (Å) and Angles (deg) for $[Fe(C_5Me_5)_2][W(C_3S_5)_3]$ (**3**)

W–S(1)	2.368(1)	S(7)–C(5)	1.737(10)
W–S(5)	2.378(1)	S(8)–C(5)	1.652(7)
W–S(6)	2.379(1)	S(9)–C(5)	1.724(9)
W–S(10)	2.379(1)	S(9)–C(6)	1.751(6)
W–S(11)	2.389(1)	S(10)–C(6)	1.737(7)
W–S(15)	2.383(1)	S(11)–C(7)	1.716(5)
S(1)–C(1)	1.702(5)	S(12)–C(7)	1.741(5)
S(2)–C(1)	1.734(4)	S(12)–C(8)	1.731(6)
S(2)–C(2)	1.718(5)	S(13)–C(8)	1.641(5)
S(3)–C(2)	1.652(5)	S(14)–C(8)	1.719(6)
S(4)–C(2)	1.723(5)	S(14)–C(9)	1.742(5)
S(4)–C(3)	1.744(5)	S(15)–C(9)	1.707(5)
S(5)–C(3)	1.712(5)	C(1)–C(3)	1.350(6)
S(6)–C(4)	1.696(6)	C(4)–C(6)	1.323(9)
S(7)–C(4)	1.751(6)	C(7)–C(9)	1.347(7)
Fe–C(11–15, 21–25)			2.093–2.108 (av 2.099)
C–C(11–15, 21–25)			1.395–1.444 (av 1.424)
$C–CH_3$(11–15:16–20, 21–25:26–30)			1.499–1.515 (av 1.504)
S(1)–W–S(5)	83.0(1)	S(5)–W–S(15)	134.8(1)
S(1)–W–S(6)	80.4(1)	S(6)–W–S(10)	82.3(1)
S(1)–W–S(10)	136.6(1)	S(6)–W–S(11)	135.2(1)
S(1)–W–S(11)	136.7(1)	S(6)–W–S(15)	81.0(1)
S(1)–W–S(15)	80.9(1)	S(10)–W–S(11)	80.8(1)
S(5)–W–S(6)	136.9(1)	S(10)–W–S(15)	134.7(1)
S(5)–W–S(10)	83.1(1)	S(11)–W–S(15)	82.1(1)
S(5)–W–S(11)	81.3(1)		

salts of the $[C_3(CN)_5]^-$, $[(NC)_2C_2(CN)_2]\cdot MeCN$,[36] $[C_4(CN)_6]^-$,[37] and $[C_6Cl_2(CN)_2(O)(OH)]^-$ anions.[38] The average Fe–C, C–C, and C–Me bond distances are 2.099, 1.424, and 1.505 Å, respectively, which are in good agreement with those of the above-mentioned $[Fe(C_5Me_5)_2]^+$ salts. The Fe atom is located at 1.715 and 1.714 Å from the C_5 rings. The Fe–C and Fe–C_5 ring centroid distances are somewhat longer than those of $Fe(C_5Me_5)_2$ (average 2.050 and 1.657 Å, respectively).[39]

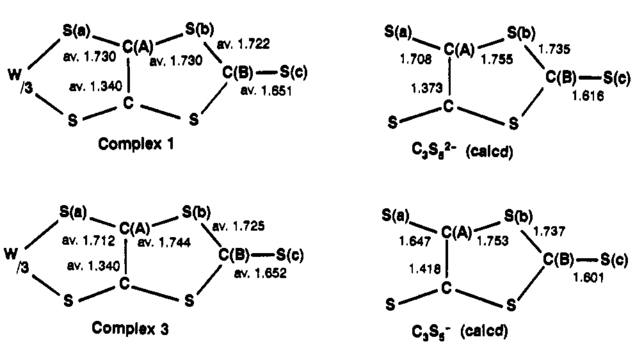

Figure 7. Bond distances for the C_3S_5 ligands of **1** and **3**, together with theoretically calculated distances for the $C_3S_5^{2-}$ and $C_3S_5^-$ moieties.

The anion moiety in which the tungsten atom is coordinated by three C_3S_5 ligands has almost a regular trigonal prismatic geometry (0° twist angle). This closely resemble those of $[Mo(S_2C_2H_2)_3]^0$ [40] and $[Mo(S_2C_6H_4)_3]^0$.[41] Although the S(1)–S(5) and the S(6)–S(10) planes are almost straight extended outside from the center of the trigonal prismatic core, the S(11)–S(15) plane is appreciably bent on the S(11) and S(15) atoms. This is caused by the intermolecular S–S nonbonded contacts of this ligand moiety through the S(11) and S(14) atoms forming an anion chain, as described below.

The average W–S distance (2.379 Å) for **3** is close to that for **1**. As illustrated in Figure 7, S(a)–C(A) distances of the C_3S_5 ligand for **3** (1.696–1.737 Å, average 1.712 Å) are appreciably shortened compared with S(b)–C(A) distances (1.734–1.751 Å, average 1.744 Å), while for **1** the S(a)–C(A) distances (1.725–1.737 Å, average 1.730 Å) are very similar to the S(b)–C(A) distances (1.723–1.737 Å, average 1.730 Å). Somewhat short S(a)–C(A) distances compared with S(b)–C(A) distances were also observed for the one-electron-oxidized $[V(C_3S_5)_3]^-$ species.[7] The ligand-centered oxidation is deduced for this anion as well as other one-electron-oxidized $[Re(C_3S_5)_3]^0$ [13] and $[Au(C_3S_5)_2]^0$ species.[42] This is also the same for the $[W(C_3S_5)_3]^-$ anion of **3** on the basis of the ESR signal and the IR C=C stretching frequency of the ligand, as described below. The reduction of the S(a)–C(A) bond distance can be theoretically estimated from the one-electron oxidation of the $C_3S_5^{2-}$ ligand moiety (Figure 7). On oxidation, the S(a)–C(A) bond is appreciably shortened while the S(b)–C(A) bond remains unvaried. Similarly, the reduction of the S–C bond was calculated for the oxidation of the benzene-1,2-dithiolate(2–) ligand.[43] Although the C–C distance is expected to be lengthened on the basis of the calculation, the C–C distances (average 1.340 Å) for **3** are almost the same as those of **1** (average 1.340 Å), the IR C=C stretching frequency being lowered for **3** with the ligand-centered oxidation compared with that of **1**.

Figure 8 shows the packing diagram of the $[W(C_3S_5)_3]^-$ anions. Some intermolecular S–S nonbonded contacts within the sum of van der Waals radii (3.7 Å, represented by dashed lines) are observed along the *b*-axis in the crystal phase: S(4)–S′(11) = 3.668, S(5)–S′(11) = 3.593, S(6)–S″(14) = 3.560 Å. From this crystal structure one-dimensional molecular interactions among the anions are deduced in spite of the bulky geometry of the

---

(37) Miller, J. S.; Zhang, J. H.; Reiff, W. M. *J. Am. Chem. Soc.* **1987**, *109*, 4584.

(38) Gerbert, E.; Reis, A. H. J.; Miller, J. S.; Rommelmann, H.; Epstein, A. J. *J. Am. Chem. Soc.* **1982**, *104*, 4403.

(39) Freyberg, D. P.; Robbins, J. L.; Raymond, K. N.; Smart, J. C. *J. Am. Chem. Soc.* **1979**, *101*, 892.

(40) Smith, A.; Schrauzer, G. N.; Mayweg, V. P.; Heinrich, W. *J. Am. Chem. Soc.* **1965**, *87*, 579.

(41) Bennett, M. J.; Cowie, M.; Martin, J. L.; Takats, J. *J. Am. Chem. Soc.* **1973**, *95*, 7504.

(42) Matsubayashi, G.; Yokozawa, A. *J. Chem. Soc., Dalton Trans.* **1990**, 3535.

(43) Cowie, M.; Bennett, M. J. *Inorg. Chem.* **1976**, *15*, 1595.

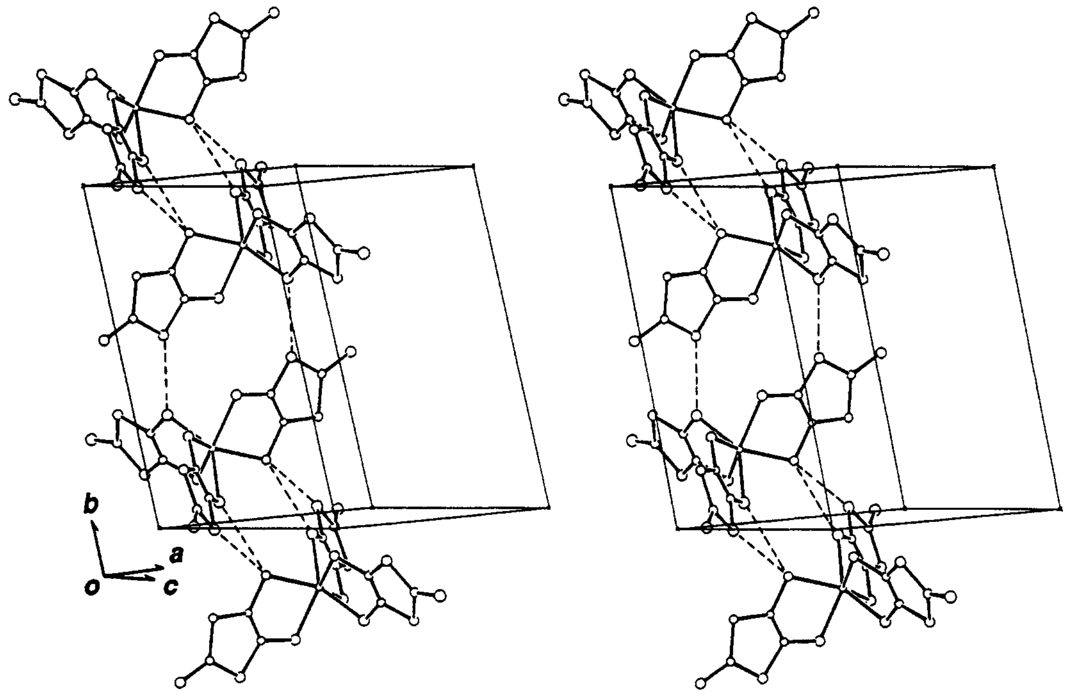

Figure 8. Stereoview of the packing diagram of the $[W(C_3S_5)_3]^-$ anions of **3**. Dashed lines represent S–S nonbonded contacts less than 3.7 Å.

Table VII. Electrical Conductivities (σ)[a]

complex	σ_{RT}, S cm^{-1}	complex	σ_{RT}, S cm^{-1}
1	6.0×10^{-8}	**7**	1.1×10^{-3}
2	3.0×10^{-8}	**8**	1.5×10^{-1}
3	6.0×10^{-5}	**9**	6.1×10^{-3}
4	1.1×10^{-4}	**10**	4.2×10^{-2}
5	1.3×10^{-3}	**11**	1.6×10^{-7}
6	3.3×10^{-3}	**12**	1.1×10^{-2}

[a] Measured for compacted pellets at room temperature.

anion. This is similar to the crystal structure of [*N*-methylphenazinium]$_2$[$V(C_3S_5)_3$].[7] The S–S interaction results in the above-mentioned broad ESR signal, and somewhat elevated electrical conductivity of this complex as described below.

Electrical Conductivities. Electrical conductivities of the complexes measured at room temperature for compacted pellets are listed in Table VII. Although complexes **1** and **2** are essentially insulators, one-electron-oxidized species **3** and **4** behave as semiconductors. In these complexes electron-conduction pathways are constructed with molecular interactions of the anion moieties through S–S contacts, as described for the crystal structure for **3**. However, complex **11** which was formed electrochemically as a one-electron-oxidized species exhibits a very small conductivity, suggesting no effective intermolecular interactions in the solid state.

The further oxidized complexes **5**–**10** and **12** exhibit high electrical conductivities. Particularly, **8**, **10**, and **12** behave as good conductors. The oxidation of the anion moieties results in more effective packing of the $[M(C_3S_5)_3]$ (M = W, Mo) moieties suitable for electron conduction, in which intermolecular contacts through the ligand-sulfur atoms can be formed owing to the major lack of amounts of bulky cations and decreased repulsions among oxidized $[M(C_3S_5)_3]^{n-}$ ($n < 2$) moieties.

Acknowledgment. We are grateful to Dr. Takamitsu Kohzuma (College of General Education, Osaka University) for the measurement of ESR spectra.

Supplementary Material Available: Full lists of crystallographic data (Table S1), bond distances and angles (Tables S2–S4), and anisotropic thermal parameters (Tables S5–S7) for **1**–**3** (8 pages). Ordering information is given on any current masthead page.